# C-band real-time 400/300 Gb/s OOK bidirectional interconnection over 20 km multicore fibers

**Zhenhua Feng (冯振华)[1], Honglin Ji (计红林)[2], Ming Tang (唐 明)[1,*], Lilin Yi (义理林)[2], Lin Gan (甘 霖)[1], Lei Xue (薛 雷)[2], Qiong Wu (吴 琼)[1], Borui Li (李博睿)[1], Jiajia Zhao (赵佳佳)[1], Weijun Tong (童维军)[3], Songnian Fu (付松年)[1], Deming Liu (刘德明)[1], and Weisheng Hu (胡卫生)[2]**

[1]*Wuhan National Lab for Optoelectronics (WNLO) & National Engineering Laboratory for Next Generation Internet Access System, School of Optical and Electronic Information, Huazhong University of Science and Technology, Wuhan, 430074, China*

[2]*State Key Laboratory of Advanced Optical Communication Systems and Network, Shanghai Jiao Tong University, Shanghai, 200240, China*

[3]*State Key Laboratory of Optical fiber and Cable Manufacture Technology, Yangtze Optical fiber and Cable Joint Stock Limited Company (YOFC), Wuhan, 430073, China*

**Corresponding author: tangming@mail.hust.edu.cn*

Received February 26, 2017; accepted April 21, 2017; posted online May 12, 2017

We experimentally demonstrate a real-time quasi-full-duplex 400G/300G optical interconnection over 20 km multicore fibers (MCFs), using 10G-class transponders operated in the C-band. Optical delay interferometer (ODI)-based optical frequency equalization is applied to mitigate chirp and dispersion induced impairments, so that the tolerance to inter-symbol interference (ISI) can be enhanced, thus enabling $4 \times 25$ Gb/s on-off keying (OOK) transmission per core over severely limited bandwidth channels. Real-time bit error ratio (BER) performances of the bidirectional 400 Gb/s transmission are measured without using extra digital signal processing (DSP) or electrical equalization, which ensures low complexity and less power consumption.

*OCIS codes: 060.0060, 060.4510, 060.2330.*
*doi: 10.3788/COL201715.080602.*

With the increasing capacity demands fueled by the emerging heterogeneous and bandwidth-intensive applications, such as cloud computing, 4K/8K videos, and virtual reality (VR), the need for low-cost, power-efficient, and high-density short-reach optical interconnects operating at 100 Gb/s and beyond has drawn significant research efforts. Although advanced modulation formats[1,2], including multi-level pulse-amplitude modulation (PAM) and discrete multi-tone (DMT), have been frequently proposed, the simplest on-off keying (OOK) with intensity-modulation and direct-detection (IM/DD) seems to be overlooked. It has been shown that OOK can cost-effectively offer good transmission performance in short-reach (~1 km) 100G optical interconnects[3] without using expensive digital-to-analog converters (DACs), analog-to-digital converters (ADCs), or complicated digital signal processing (DSP). However, the high baud-rate OOK signal aggravates the bandwidth requirement of electrical components and restricts the transmission distance due to dispersion. In order to extend the transmission reach, multi-lanes of lower-baud-rate parallel tributaries can be exploited by stacking multiple wavelength channels into one optical fiber through the coarse wavelength division multiplexing (WDM)[4,5].

On the other hand, as bidirectional transmission is ubiquitous in tremendously high-density fiber cable connections between servers and racks in data centers, a space congestion problem may happen. Therefore, reducing the physical footprint of the optical interconnects is especially important. Traditionally, separate optical fibers are used as full-duplex channels in a bidirectional transmission. Tempted by the advantages of high-density spatial channel count, integration compatibility, and lowcost, space division multiplexing (SDM) technologies based on novel fibers[6–8] have been exploited to enhance the fiber capacity in short-range optical communication systems with IM/DD. Few mode fibers (FMFs) can accommodate several spatial channels using orthogonal mode division multiplexing (MDM) to support large capacity transmission with the help of computationally intensive multiple input multiple output (MIMO) DSP to equalize the modal crosstalk[9], otherwise, specially designed and fabricated low-crosstalk FMF is required[7,8]. Besides, the attainable spatial channel counts and the corresponding mode multiplexer/demultiplexer with low crosstalk and insertion loss may be another obstacle before its deployment in cost-sensitive optical interconnection scenarios. Instead, the multicore fiber (MCF) is considered to be a better choice that is suitable for high-speed optical interconnections, owing to its well-controlled inter-core crosstalk and almost identical transmission quality compared with standard single mode fibers (SSMFs). A six-channel parallel MCF interconnection using 850 nm multimode vertical cavity surface emitting lasers is demonstrated with an aggregate capacity of 120 Gb/s[10]. An 800 Gb/s per fiber O-band transmission is also reported based on a

 

125-μm-cladding eight-core fiber using electro-absorption modulated lasers (EMLs) and praseodymium-doped fiber amplifier (PDFA)[11]. However, the transmission distances reported in these works are quite limited (≤2 km) due to large fiber loss and unavailable fiber amplifiers at the shorter wavelengths. To support the next generation 400G interconnections with longer reach (≥10 km), like large-scale datacenter networks, lower fiber attenuation and commercial fiber amplifier are indispensable, which makes the C-band more competitive despite certain chromatic dispersions. Using our own designed and fabricated hexagonal seven-core MCF and in-house developed compact fan-in/fan-out devices, we have demonstrated an MCF enabled wavelength and SDM (WSDM) optical access network with a large capacity (>300 Gb/s) and long reach (~58 km)[12,13].

In this work, we further utilized the MCF-SDM scheme to demonstrate a quasi-full-duplex 400 Gb/s C-band OOK bidirectional transmission over a 20 km seven-core fiber, using 10G-class transceivers without any DSP or electrical equalization. To address the frequency selective power fading induced by the laser chirp and fiber dispersion, an optical delay interferometer (ODI) is employed as an optical equalizer for all four wavelength channels, which enables open and clear eyes even after a 20 km MCF transmission.

As shown in Fig. 1, in the transmitter (TX) side, four 1.6 nm spaced C-band wavelengths emitted from four directly modulated lasers (DMLs) are intensity modulated by four independent 25 Gbaud pseudorandom binary sequences (PRBSs) generated from the pulse pattern generator (PPG, Keysight N4960 A). The DMLs are commercially available products with a 10 dB modulation bandwidth of about 10 GHz. The low-cost and low-bandwidth transceivers are one of the major limiting factors to get the achievable performance in short-range cost-sensitive communication systems. Especially in high-speed direct modulation cases, the modulation

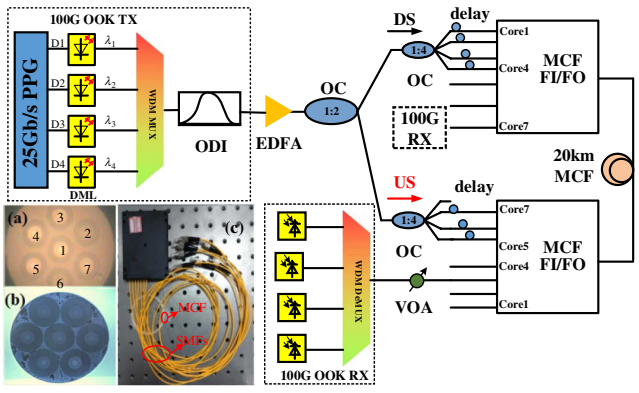


Fig. 1. Experimental setup of bidirectional MCF transmission system. The insets (a), (b), and (c) are the cross section view of the fabricated MCF, fan-in/fan-out, and picture of the whole fan-in/fan-out device, respectively. (OC, optical coupler; FI/FO, fan-in/fan-out; RX, receiver; Mux, multiplexer; DeMux, demultiplexer.)

induced frequency chirp is non-negligible, which needs pre-equalization or post-compensation, otherwise inter-symbol interference (ISI) occurs. Inspired by the chirp management method[14,15], an ODI is applied to the OOK modulated signals to combat the distortions resulted from laser chirp and fiber dispersion. As an optical frequency equalizer, the notch band of the ODI should be aligned to the optical sideband with the longer wavelength so as to equalize frequency fading and alleviate the ISI. The free spectral range (FSR) of the ODI is 66.67 GHz, thus, it can be simultaneously accommodated for all four 200 GHz spaced signal channels. The WDM signal output from the TX is first power amplified by an erbium-doped fiber amplifier (EDFA) and then divided into two branches; one is for downstream (DS) transmission, and the other is used as upstream (US) traffic. After that, each of the split signals is further power split into four tributaries with different time delays for spatial channel decorrelation. For the DS transmission, four decorrelated WDM signals are correspondingly launched into four cores of the MCF via a low crosstalk and low-loss fan-in device. As shown in Fig. 1(c), the homemade fan-in/fan-out device has a compact size, one end of which is fusion spliced to the MCF, and the other end is split and connected to seven individual single mode fiber (SMF) pigtails. Since the MCF we used is a seven-core fiber, only three cores can be used to support the US transmission in the opposite direction for this demonstration, nevertheless, specially designed and fabricated eight-core fibers can be used to achieve a full-duplex 400G bidirectional transmission[11,16].

After 20 km MCF transmission, the spatial channels are demultiplexed by another fan-in/fan-out device so that the 100 Gb/s OOK signal in each core can be adapted to an SMF. For each of the spatial channels, a WDM demultiplexer follows to separate and extract the individual 25 Gb/s spectral channels. In order to adjust the received optical power (ROP), a variable optical attenuator (VOA) is inserted before the receiver. For each wavelength, a 10G-class PIN photodetector (PD) is used to detect the 25 Gb/s per $\lambda$ OOK signal. As the modulation format in this experiment is OOK, no extra DSP or electrical equalization is required, which can help to reduce the complexity and power consumption of the transceivers, thus, the latency decreases. Real-time transmission performance in terms of eye diagrams and bit error ratio (BER) can be obtained directly by the off-the-shelf bit-error tester (BERT, MultiLane ML4009). Due to the limitation of our experimental instruments, all of the spatial and spectral channels under test in the DS and US are simultaneously transmitted, but they are detected and recovered one by one.

During the experiments, first, we measured the end-to-end insertion loss of our MCF link, including a pair of fan-in/fan-out devices and 20 km MCFs. The main parameters for the design and fabrication of the MCF and fan-in/fan-out can be found in our previous work[12]. With an optimized manufacturing process, the performances of our fabricated seven-core fiber and fan-in/fan-out devices

have been improved a lot. The average loss per core is about 7 dB, and the inter-core crosstalk is less than −45 dB per 100 km, which is low enough for SDM transmission. The chromatic dispersion parameter of our fabricated MCF is comparable with that of an SMF and other optical parameters, including zero dispersion wavelength, mode field diameter, and bending loss, which can be found in our recent work[17].

Then, we turned on DML 1, while keeping the other three DMLs off, and measured the optical spectra of the DS OOK signals with and without ODI in the optical back-to-back (OB2B) case. With careful alignment of the center wavelength of the DML, one of the notch bands of the ODI can be well-fitted to the long wavelength sideband of the OOK signal. Of course, this procedure can be further optimized to acquire a better eye diagram. As shown in Fig. 2, after filtering by the ODI, the spectrum of the directly modulated OOK signal experiences strong spectral shaping in the long wavelength sideband, which corresponds to the long wavelength part of the optical signal induced by the red-shift chirp. In that case, the '0's in the data sequence are suppressed, thus, the extinction ratio can be improved[18,19]. As a result, the eye diagram opens clearly, which means an enhanced resistance to the ISI effect induced by bandwidth limitation, laser chirp, and dispersion.

To further demonstrate the frequency equalization effect of the ODI, we also measured the OB2B frequency response of the transceivers with and without ODI using a vector network analyzer (VNA). Figure 3 shows the measured frequency responses of the DML and PIN. Due to the limited bandwidth of the transceivers, the frequency response within the cut-off frequency drops rapidly in the absence of ODI even in the OB2B case, and the resultant 3 dB bandwidth is about 3 GHz. Fortunately, with the help of ODI, we observe that the high-frequency response is improved significantly and the 3 dB bandwidth of the OB2B system extends to more than 11 GHz thanks to the ODI-based chirp management and frequency equalization effect.

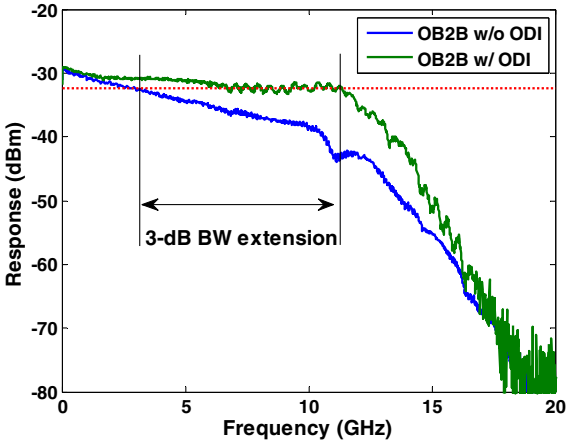


Fig. 3. (Color online) Frequency response of the transceivers with and without ODI. (BW, bandwidth.)

Subsequently, we turned on all the four DMLs with the channel spacing setting to 200 GHz and then modulated them with independent 25 Gb/s OOK signals under the condition of a proper bias current and driving voltage. Optical spectra of the four wavelength multiplexed 100 Gb/s OOK signals after ODI spectral shaping are shown in Fig. 4. We can see that all four wavelengths in C-band are with equal optical power, and the side mode suppression ratios (SMSRs) for all of the DMLs are higher than 45 dB. To avoid the fiber nonlinearity, the total launching power for each core is controlled at about 14 dBm for four wavelengths.

In order to evaluate the transmission performance of the whole system, we first checked the role of ODI on the eye diagram of OB2B and MCF transmission. As shown in Fig. 5, in OB2B case, four wavelength channels perform similarly no matter whether ODI is used. The OB2B eye diagrams for 25 Gb/s OOK signals are not quite open and look like duobinary (DB) ones because of the ISI

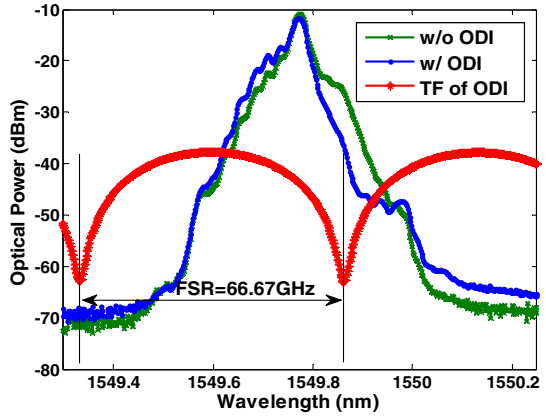


Fig. 2. (Color online) Spectrum of 25 Gb/s OOK signal generated by DML1 with and without ODI, the transmission function of the ODI is also depicted. (w/o, without; w/, with; TF, transmission function.)

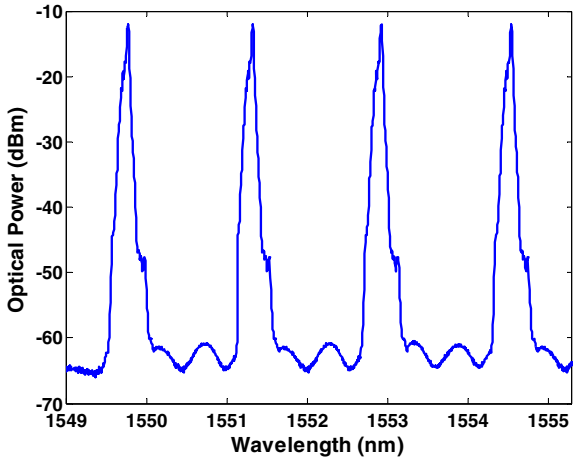


Fig. 4. Optical spectra of the WDM multiplexed 100 Gb/s OOK signals after ODI filtering.

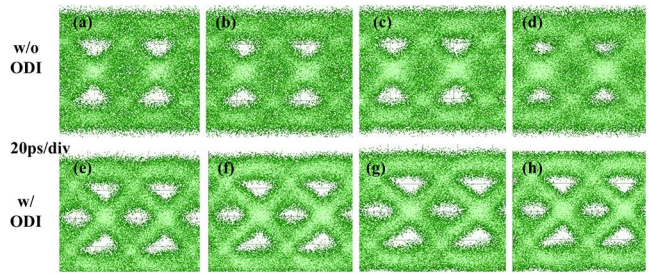


Fig. 5. Measured eye diagrams for the OB2B case with and without ODI. (a)–(d) are for $\lambda_1 \sim \lambda_4$ without ODI, and (e)–(h) are for $\lambda_1 \sim \lambda_4$ with ODI, respectively.

induced by the chirp and bandwidth limited transponders. Fortunately, the ODI introduced in the TX can be viewed as an optical equalizer, which helps to reduce the ISI for all four spectral channels simultaneously. After the 20 km MCF transmission, the OOK eye diagrams were completely closed without using ODI due to the dispersion induced degradation. We also see that the improvement enabled by the ODI equalization becomes more significant in the presence of chromatic dispersion. The eye diagrams of $\lambda_1$ for core 1 in the DS direction without and with ODI are shown in Figs. 6(a) and 6(c), while eye diagrams of $\lambda_2$ for core 5 in the US direction without and with ODI are shown in Figs. 6(b) and 6(d), respectively.

Lastly, we investigated the BER performance versus different ROPs for the bidirectional transmission system when ODI is used in the TX. Cores 1 to 4 are used for DS, while cores 5 to 7 are for US transmission. As a result, the aggregate data rate per fiber is 700 Gb/s, in which 400 Gb/s (4 SDM × 4 WDM × 25 Gb/s) is for DS, while 300 Gb/s is for US. With higher spatial-channel-count MCFs, large-capacity full-duplex transmission can be realized with a symmetric data rate. All the spectral

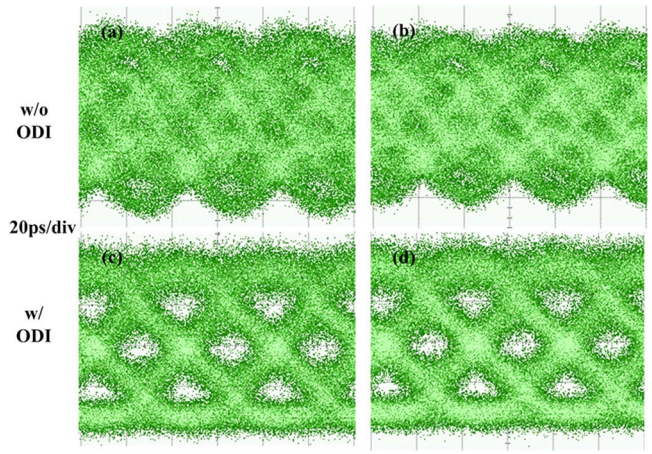


Fig. 6. Measured eye diagrams of 25G OOK signals after 20 km MCF transmission. (a) $\lambda_1$ in core 1 for the DS direction without ODI, (b) $\lambda_2$ in core 5 for the US direction without ODI, (c) $\lambda_1$ in core 1 for the DS direction with ODI, (d) $\lambda_2$ in core 5 for the US direction with ODI.

and spatial channels were tested successively, and the measured BER performances of 100G OOK signals over 20 km MCF transmission for DS (cores 1 and 2) and US (cores 5 and 6) are shown in Fig. 7. It can be seen that all the 25 G/s OOK subchannels have similar receiver sensitivity of about −13 dBm to reach the FEC limit at BER $= 3.8 \times 10^{-3}$, offering more than a 10 dB loss budget. The receiver sensitivity variation among all of the spectral and spatial channels is also investigated, and the results are summarized in Fig. 8, from which we can see that the maximum variation is about 1.5 dB due to the DML wavelength drifts and heterogeneous fiber core parameters. The relatively larger sensitivity variation for DS in cores 1–4 is mainly caused by the transmission direction related insertion loss and end face reflection of our fabricated fan-in/fan-out devices in the MCF link. The experimental result proves the feasibility of using

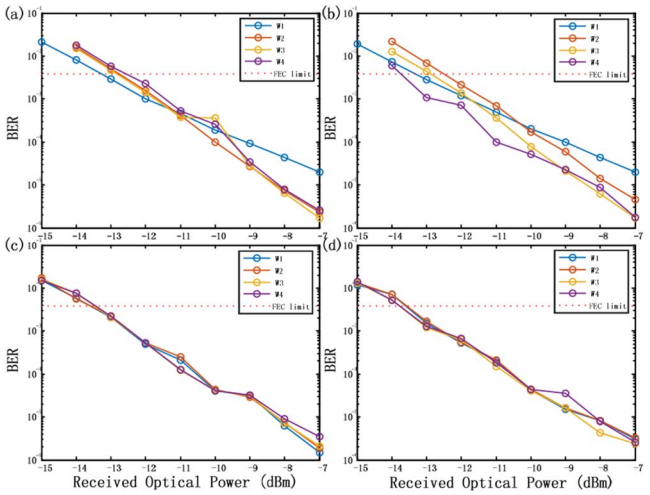


Fig. 7. (Color online) BER performances of 100G OOK signals for different cores in bidirectional MCF transmission. (a)–(d) are for DS (core 1 and 2) and US (core 5 and 6), respectively. ($W_1 - W_4$: $\lambda_1 - \lambda_4$.)

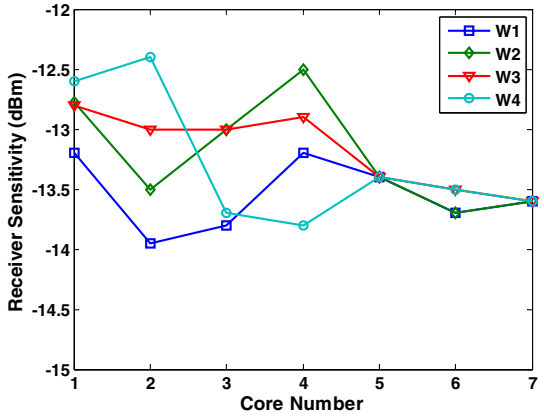


Fig. 8. Receiver sensitivity variation among different fiber cores and wavelengths. ($W_1 - W_4$: $\lambda_1 - \lambda_4$.)

10G-class transceivers to support C-band quasi-duplex 400 Gb/s transmission with the aid of spatial channel multiplexing over wavelength channel stacking and ODI-based optical domain equalization.

In conclusion, taking advantage of spatial channel multiplexing over wavelength stacking, we experimentally demonstrate a real-time quasi-full-duplex 400G/300G optical interconnection over 20 km MCFs, using only 10G-class transponders operated in the C-band. To address the bandwidth limited problem, which can be further aggravated by chirp and dispersion, we utilize a single ODI as an optical frequency equalizer for all four wavelength channels simultaneously. With this technique, the 3 dB bandwidth of transponders can be greatly extended, and the quality of the eye diagrams can be significantly improved. Thanks to the ODI-based chirp management and frequency equalization, 100 Gb/s per fiber core transmission can be realized with a receiver sensitivity of about −13 dBm. Owing to the mitigation of complex DSP and electrical equalization, real-time recording of BER for the quasi-full-duplex bidirectional 400 Gb/s transmission is achieved, enabling cost-efficient large-capacity optical interconnection with low complexity and power consumption. Receiver sensitivities of all of the spectral and spatial channels are measured, and the maximum sensitivity variation is found to be around 1.5 dB.

With the emerging of heterogeneous and bandwidth-intensive applications driven by the upcoming era of 5G and internet of things (IOT), large-capacity short-reach optical interconnection operating at 100 Gb/s and beyond is highly desired. To support such a scenario, inherently high-density and potentially cost-efficient SDM technologies are indispensable. Considering the space congestion problem, which may happen among the massive connections between servers and racks in data centers, the MCF will play as an important and promising transmission media to support high-density bidirectional optical interconnection. With the development of low-crosstalk MCF and compact low-loss fan-in and fan-out devices, more spatial channels can be feasible in one pipeline, thus, it emerges as an ideal platform for future data-driven multi-service featured high-density optical interconnections. As an alternative, FMF is also a promising physical medium for big-data services transmission with technical progress on low-crosstalk FMF fabrication and low-loss mode multiplexing and demultiplexing techniques. Ultimately, dense SDM technologies using multicore FMFs are expected to further enhance the capacity by orders of magnitude, supporting even larger bandwidth transmissions with a lower system cost. For the short-range transmission scenario, the use of 10G-class transceivers is also important to control the system cost while upgrading the capacity. It is envisaged that the extensively studied PAM4 transmission techniques can be easily applied to our MCF system to further improve the DS/US capacity to 800 Gb/s with the help of some essential DSP algorithms during PAM4 signal modulation and demodulation.

This work was supported by the National Natural Science Foundation of China (Nos. 61331010 and 61205063), the National 863 Program of China (No. 2015AA016904), and the Program for New Century Excellent Talents in University (No. NCET-13-0235).

## References

1. K. Zhong, X. Zhou, T. Gui, L. Tao, Y. Gao, W. Chen, J. Man, L. Zeng, A. P. T. Lau, and C. Lu, Opt. Express **23**, 1176 (2015).
2. Z. Wang, L. Tao, Y. Wang, and N. Chi, Chin. Opt. Lett. **13**, 080602 (2015).
3. J. Lee, N. Kaneda, T. Pfau, A. Konczykowska, F. Jorge, J.-Y. Dupuy, and Y.-K. Chen, in *Optical Fiber Communication Conference* (2014), Th5A.5.
4. S. J. Trowbridge, in *Optical Fiber Communications Conference and Exhibition (OFC)* (2015), 1.
5. Z. Zhang, X. Jiang, J. Wang, X. Chen, and L. Wang, Chin. Opt. Lett. **13**, 020603 (2015).
6. B. Zhu, T. Taunay, M. Yan, J. Fini, M. Fishteyn, E. Monberg, and F. Dimarcello, Opt. Express **18**, 11117 (2010).
7. G. Milione, P. Ji, E. Ip, M.-J. Li, J. Stone, and G. Peng, in *Optical Fiber Communications Conference and Exhibition (OFC)* (2016), 1.
8. F. Ren, J. Li, T. Hu, R. Tang, J. Yu, Q. Mo, Y. He, Z. Chen, and Z. Li, IEEE Photon. J. **7**, 1 (2015).
9. R. Ryf, S. Randel, A. H. Gnauck, C. Bolle, A. Sierra, S. Mumtaz, M. Esmaeelpour, E. C. Burrows, R.-J. Essiambre, and P. J. Winzer, J. Lightwave Technol. **30**, 521 (2012).
10. B. G. Lee, D. M. Kuchta, F. E. Doany, C. L. Schow, P. Pepeljugoski, C. Baks, T. F. Taunay, B. Zhu, M. F. Yan, and G. E. Oulundsen, J. Lightwave Technol. **30**, 886 (2012).
11. T. Hayashi, T. Nakanishi, K. Hirashima, O. Shimakawa, F. Sato, K. Koyama, A. Furuya, Y. Murakami, and T. Sasaki, J. Lightwave Technol. **34**, 85 (2016).
12. B. Li, Z. Feng, M. Tang, Z. Xu, S. Fu, Q. Wu, L. Deng, W. Tong, S. Liu, and P. P. Shum, Opt. Express **23**, 10997 (2015).
13. Z. Feng, B. Li, M. Tang, L. Gan, R. Wang, R. Lin, Z. Xu, S. Fu, L. Deng, and W. Tong, IEEE Photon. J. **7**, 1 (2015).
14. S. Zhou, X. Li, L. Yi, Q. Yang, and S. Fu, Opt. Lett. **41**, 1805 (2016).
15. Z. Li, L. Yi, X. Wang, and W. Hu, Opt. Express **23**, 20249 (2015).
16. J. K. Mishra, B. Rahman, and V. Priye, IEEE Photon. J. **8**, 1 (2016).
17. Z. Feng, L. Xu, Q. Wu, M. Tang, S. Fu, W. Tong, P. P. Shum, and D. Liu, Opt. Express **25**, 5951 (2017).
18. S.-C. Lin, S.-L. Lee, and C.-L. Yang, J. Opt. Networking **8**, 306 (2009).
19. Z. Zhou, M. Bi, S. Xiao, Y. Zhang, and W. Hu, IEEE Photon. Technol. Lett. **27**, 470 (2015).